1.0	4.5	2.8	2.5
		3.2	2.2
		3.6	
1.1	4.0		2.0
			1.8
1.25	1.4		1.6

MICROCOPY RESOLUTION TEST CHART
NATIONAL BUREAU OF STANDARDS 1963 A

REPORT DOCUMENTATION PAGE		READ INSTRUCTIONS BEFORE COMPLETING FORM
1 REPORT NUMBER NRL Memorandum Report 4758	2 GOVT ACCESSION NO.	3 RECIPIENT'S CATALOG NUMBER
4 TITLE (and Subtitle) A COMPARISON OF MICROSTRUCTURAL EFFECTS ON FATIGUE-CRACK INITIATION AND PROPAGATION IN Ti-6Al-4V		5 TYPE OF REPORT & PERIOD COVERED Final report on one phase of a continuing NRL problem.
		6 PERFORMING ORG REPORT NUMBER
7 AUTHOR(s) G. R. Yoder, L. A. Cooley, and T. W. Crooker		8 CONTRACT OR GRANT NUMBER(s)
9 PERFORMING ORGANIZATION NAME AND ADDRESS Naval Research Laboratory Washington, DC 20375		10 PROGRAM ELEMENT PROJECT, TASK AREA & WORK UNIT NUMBERS 61153N; WR022-01-01; 63-1054-0-2
11 CONTROLLING OFFICE NAME AND ADDRESS Naval Air Systems Command Office of Naval Research Washington, DC 20361 Arlington, VA 22217		12 REPORT DATE March 5, 1982
		13 NUMBER OF PAGES 16
14 MONITORING AGENCY NAME & ADDRESS(if different from Controlling Office)		15 SECURITY CLASS (of this report) UNCLASSIFIED
		15a DECLASSIFICATION DOWNGRADING SCHEDULE

16 DISTRIBUTION STATEMENT (of this Report)

Approved for public release; distribution unlimited.

17 DISTRIBUTION STATEMENT (of the abstract entered in Block 20, if different from Report)

19 KEY WORDS (Continue on reverse side if necessary and identify by block number)

Fatigue (materials)	Microstructure
Crack initiation	Notch stress fatigue
Crack propagation	Fracture mechanics
Titanium alloys	

20 ABSTRACT (Continue on reverse side if necessary and identify by block number)

Fatigue-crack initiation and propagation studies were conducted on commercial purity (0.20 weight percent interstitial oxygen) Ti-6Al-4V rolled plate, heat treated to produce three differing microstructures. The three heat treatments were an as-received mill anneal (MA), a recrystallization anneal (RA), and a beta anneal (BA). The fatigue-crack propagation results show a distinct ordering of crack growth rate (da/dN) versus stress-intensity range (ΔK) curves on the basis of microstructure. The coarse-grained Widmanstatten BA material exhibits the greatest resistance to crack propagation, and the

(Continues)

DD FORM 1473 1 JAN 73   EDITION OF 1 NOV 65 IS OBSOLETE
S/N 0102-014-6601

20. ABSTRACT (Continued)

finer-grained MA material offers the least crack propagation resistance. For fatigue-crack initiation, results obtained from blunt-notch WOL-type fracture mechanics specimens reveal a different ordering in relation to microstructure. The MA and RA materials are indistinguishable in their resistance to crack initiation; moreover, their crack initiation resistance is moderately superior to that of the BA material in the low-cycle regime (i.e., less than 10^5 cycles to crack initiation). However, at approximately 10^6 cycles to crack initiation, the fatigue resistance of the BA material appears equivalent to that of the MA and RA materials. In the crack initiation specimens, a theoretical stress concentration factor (K_t) of 4.1 was used. This corresponds to K_t values determined for titanium alloy jet engine components. The influence of surface roughness in the crack initiation region of blunt-notch specimens was examined; no difference in cycles-to-initiation behavior was observed for 16 and 72 μ-in. finishes, regardless of microstructure.

CONTENTS

Accession For

NTIS GRA&I
DTIC TAB
Unannounced
Justification

By
Distribution/

Availability Codes

Dist   and/or
         Special

A COMPARISON OF MICROSTRUCTURAL EFFECTS ON FATIGUE-CRACK INITIATION AND PROPAGATION IN Ti-6Al-4V

G. R. Yoder, L. A. Cooley and T. W. Crooker

Mechanics of Materials Branch
Material Science and Technology Division
Naval Research Laboratory
Washington, DC 20375

INTRODUCTION

The fatigue failure process for many structural components involves a crack initiation phase followed by a crack propagation phase. Thus, efforts to metallurgically optimize the fatigue life of structural alloys must consider both crack initiation and propagation resistance.

In this investigation, direct comparisons are made between crack initiation and crack propagation in a single plate of Ti-6Al-4V material. The material is a commerical purity alloy containing 0.20 weight percent interstitial oxygen. It was heat treated to produce three differing microstructures: an as-received mill anneal (MA), a recrystallization anneal (RA) and a beta anneal (BA). A similar specimen type is used for both crack initiation and crack propagation studies. All fatigue specimens have a common orientation with respect to the rolling direction of the plate. In this manner, it is anticipated that valid comparisons can be made between crack initiation and crack propagation behavior with a minimum of ambiguity. The crack propagation data used in these comparison are taken from the results of a previous study [1].

BACKGROUND

Fatigue-crack initiation and propagation in Ti-6Al-4V can be strongly influenced by microstructure [2-9]. In the case of crack propagation, a comprehensive understanding of microstructural effects has recently been developed. It is apparent that a single microstructural parameter, mean effective grain size ($\bar{\ell}$), plays a dominant role in controlling fatigue crack growth rates in numerous $\alpha + \beta$ titanium alloys [9]. Clearly defined trends have been established between increased resistance to fatigue crack

propagation and microstructural coarsening (i.e., crack growth rates vary inversely with $\bar{l}$).

It is also apparent that grain size plays an important, but poorly defined, role in the fatigue-crack initiation resistance of Ti-6Al-4V materials. Considerable ambiguity exists as to the specific effects of microstructure, per se, on crack initiation in these materials [2]. One source of ambiguity can be texture. Texture can exert a very strong influence on the cycles-to-failure (i.e., initiation plus propagation) fatigue life of $\alpha + \beta$ titanium alloys [10]. But, it can be very difficult to separately identify effects arising from changes in microstructure when changes in texture can also accompany micro-structural changes. Peters et al. have attempted to address this problem by varying grain size while texture remains constant [8]. Their findings on Ti-6Al-4V, which include both cycles-to-failure fatigue life and crack propagation, show that grain size refinement is beneficial to the fatigue life of smooth specimens but is detrimental to crack growth rates. The findings of Peters et al. for fatigue life are in general agreement with several studies relating forging and heat treatment variables to cycles-to-initiation fatigue life [3] and cycles-to-failure fatigue life [4, 5] for Ti-6Al-4V. However, Bowen and Stubbington noted that grain-size refinement achieved through $\alpha + \beta$ working of Ti-6Al-4V bars was more effective in increasing low-cycle fatigue life [5]. Also, Lucas showed that the effect of grain size on fatigue life was much more pronounced for notched specimens than for smooth specimens [4]. The overall conclusion regarding crack initiation points to an inverse relationship between $\bar{l}$ and fatigue life for Ti-6Al-4V materials, but the degree to which crack initiation is affected by grain size and what regime of fatigue behavior (low-cycle versus high-cyle) is most affected remains unanswered.

MATERIALS AND HEAT TREATMENTS

The Ti-6Al-4V alloy studied was in the form of a 25.4-mm thick rolled plate. Chemical analysis of the plate appears in Table I. Procedures followed in the three heat treatments are given in Table 2. Tensile properties and plane strain fracture toughness (K_{Ic}) values for each heat treatment are tabulated in Table 3. Tensile properties for the transverse (T) and longitudinal (L) orientations are provided for comparison, as an index of the degree of texture which exists for each heat-treated condition. K_{Ic} values are for the TL orientation [11].

Table 1 Chemical Composition (wt. %)						
O	Al	V	Fe	N	C	H
0.20	6.7	4.3	0.10	0.011	0.03	0.006

Table 2 Heat Treatments	
Mill Anneal (MA)	(788°C/I hr + AC), as received
Recrystallization Anneal (RA)	(954°C/4 hr + HC @ 180°C/hr to 760°C + HC @ 370°C/hr to 482°C + AC)
Beta Anneal (BA)	(1038°C/½ hr + AC) + (732°C/2 hr + AC)

HC = helium purge in vacuum furnace
AC = air cooling

Table 3 Mechanical Properties						
Heat Treatment	Fracture Toughness K_{Ic} ($MP\sqrt{a \cdot m}$)	0.2% Yield Strength σ_{ys} (MPa) T L	Tensile Strength σ_{uts} (MPa) T L	Young's Modulus E (GPa) T L	% reduction in area T L	% elongation (51-mm G.L.) T L
MA	40	1007 948	1034 986	130 118	29 26	14 15
RA	76	931 898	1007 982	130 119	26 26	15 15
BA	87	869 892	958 960	117 119	16 23	11 16

Microstructures for each heat treatment are shown in Fig. I. The MA microstructure is characterized by elongated primary alpha, the RA is equiaxed, and the BA is acicular Widmanstätten. Values of $\bar{l}$ are 5, 9, and 24 μm, respectively.*

EXPERIMENTAL PROCEDURES

Fatigue-crack propagation, fracture toughness and tensile tests were all carried out in general accordance with ASTM standards [11-13]. Crack propagation and fracture toughness data were generated using 25-mm thick IT WOL-type fracture mechanics specimens with the crack path in the TL orientation. Tensile data were generated using 12.8-mm dia. specimens.

---

*In the case of the BA microstructure, the effective grain size (24 μm) is that of the Widmanstätten colony rather than the individual platelet.
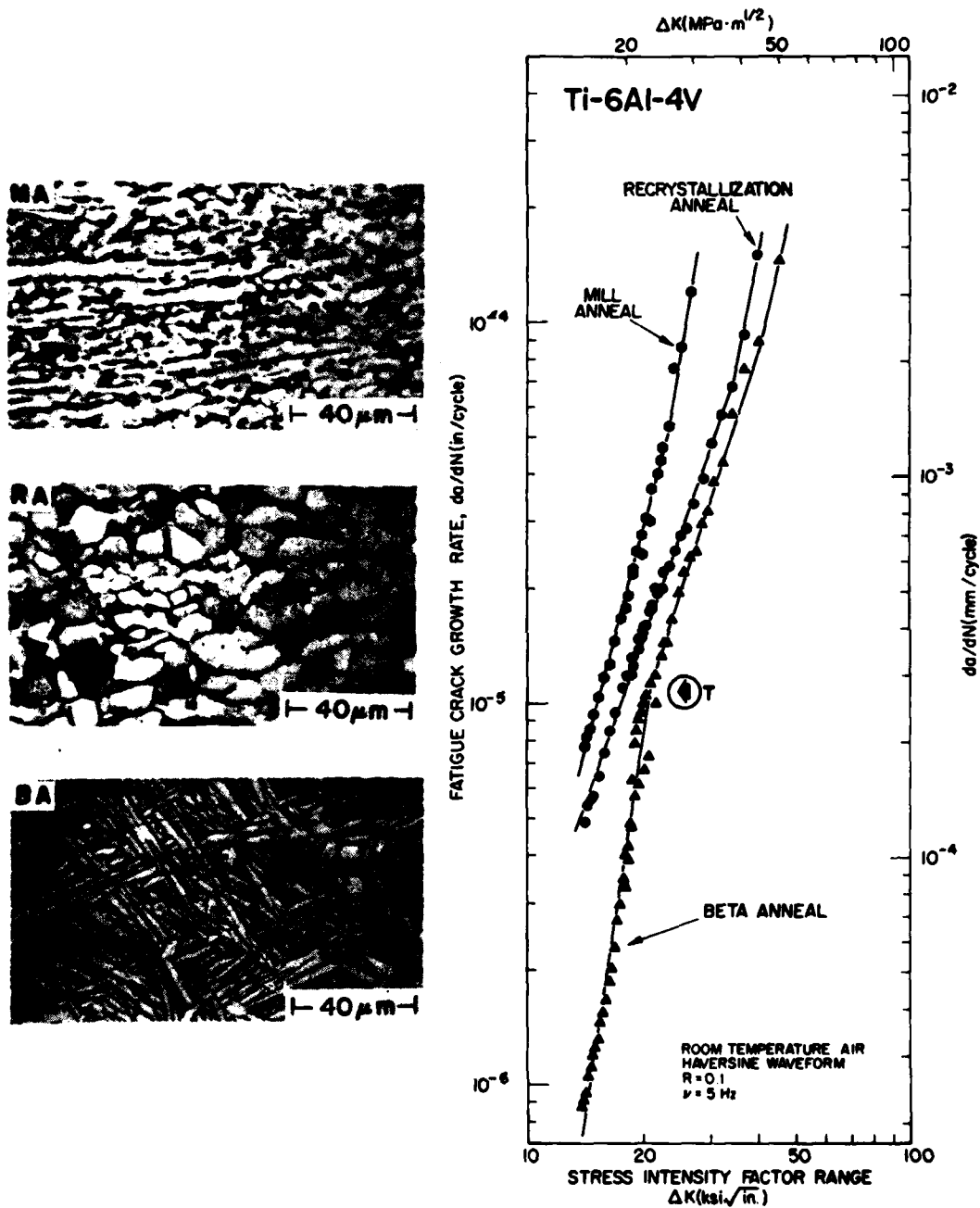
Fig. 1 - Fatigue-crack propagation results and microstructures for the three Ti-6Al-4V materials studied.

Fatigue-crack initiation data were obtained from blunt-notch WOL specimens shown in Fig. 2. Blunt-notch fracture mechanics specimens have been successfully utilized for fatigue-crack initiation of steels in recent years [14-18]. However, this investigation may mark the first use of this test method for titanium alloys.

Fatigue-crack initiation in notched members is controlled by local strains at the notch root. A number of approaches have been developed for calculating local notch-tip stresses and strains from nominal stress and notch geometry considerations. One such approach utilizes the parameter $\Delta K/\sqrt{P}$, where ΔK is the fracture mechanics stress-intensity range and P is the notch root radius. The parameter $\Delta K/\sqrt{P}$ has been shown to correlate with local notch-tip strain and provide a means of normalizing cycles-to-initiation data for various notch-tip geometries.

The relationship between the local stress range at the notch-tip ($\Delta\sigma_{max}$) and $\Delta K/\sqrt{P}$ is as follows:

$$\Delta\sigma_{max} = \frac{2(\Delta K)}{\sqrt{\pi P}}. \tag{1}$$

For the WOL specimen, the nominal stress range at the notch-tip ($\Delta\sigma_n$) is given by:

$$\Delta\sigma_n = \frac{\Delta P}{B(W-a)}\left[1 + 3\left(\frac{W+a}{W-a}\right)\right] \tag{2}$$

where ΔP is the load range, B is the specimen thickness, W is the specimen width measured from the load line, and $\underline{a}$ is the crack depth measured from the load line.

The theoretical elastic stress concentration factor (K_t) can be calculated by taking the ratio of σ_{max}/σ_n for a given specimen geometry and load range. For the specimen used in this investigation, as shown in Fig. 2 using $P = 1.6$ mm, $K_t = 4.1$. This approximates K_t values determined for titanium alloy jet engine components [19]. Concern for fatigue damage in such components provided the original stimulus for this investigation.

Fatigue-crack initiation was monitored by observation of the region of maximum stress at the notch root using a low power optical microscope. The crack initiation data, plotted in Figs. 3-5, denote crack lengths across the face of the notch for the first and last of a series of successive observations for each specimen. Generally, the method was successsful in detecting the incipient stages of visible fatigue crack formation. However, considerable diligence and a degree of good fortune is required during fatigue testing to actually observe minute fatigue cracks before they rapidly propagate across the face of the notch.
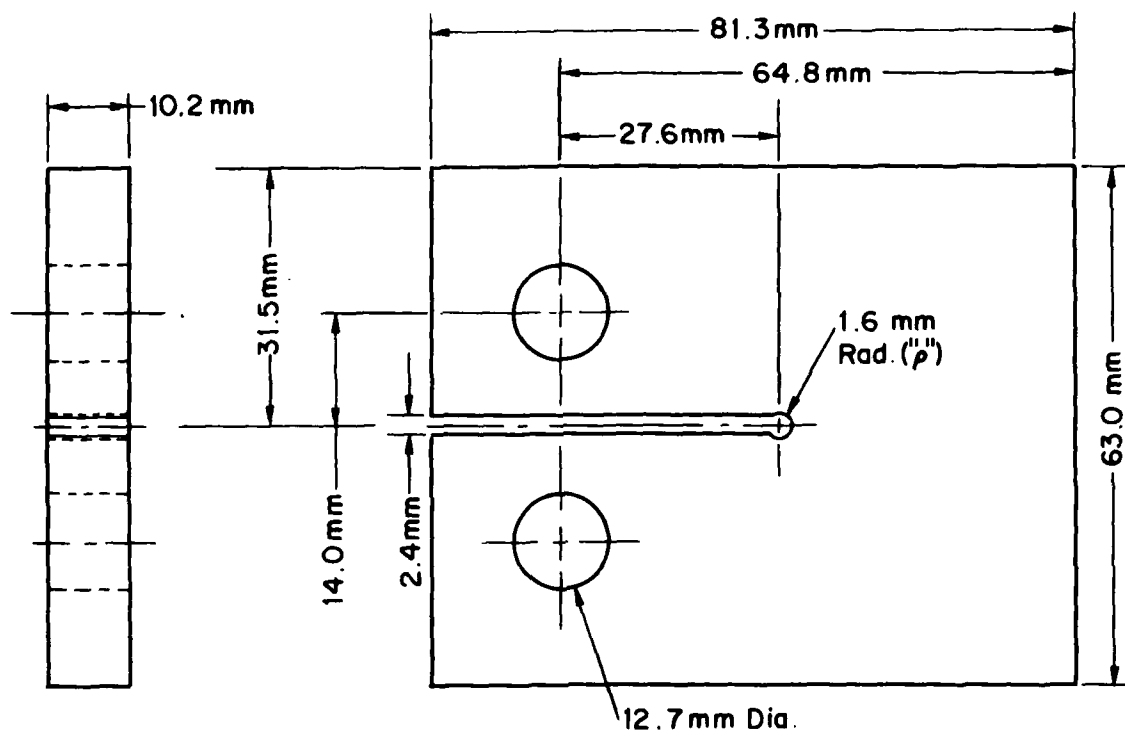
Fig. 2 - IC-mm thick blunt-notch WOL specimen used to obtain fatigue-crack initiation $(\Delta K/\sqrt{\rho}$-vs-N) data.
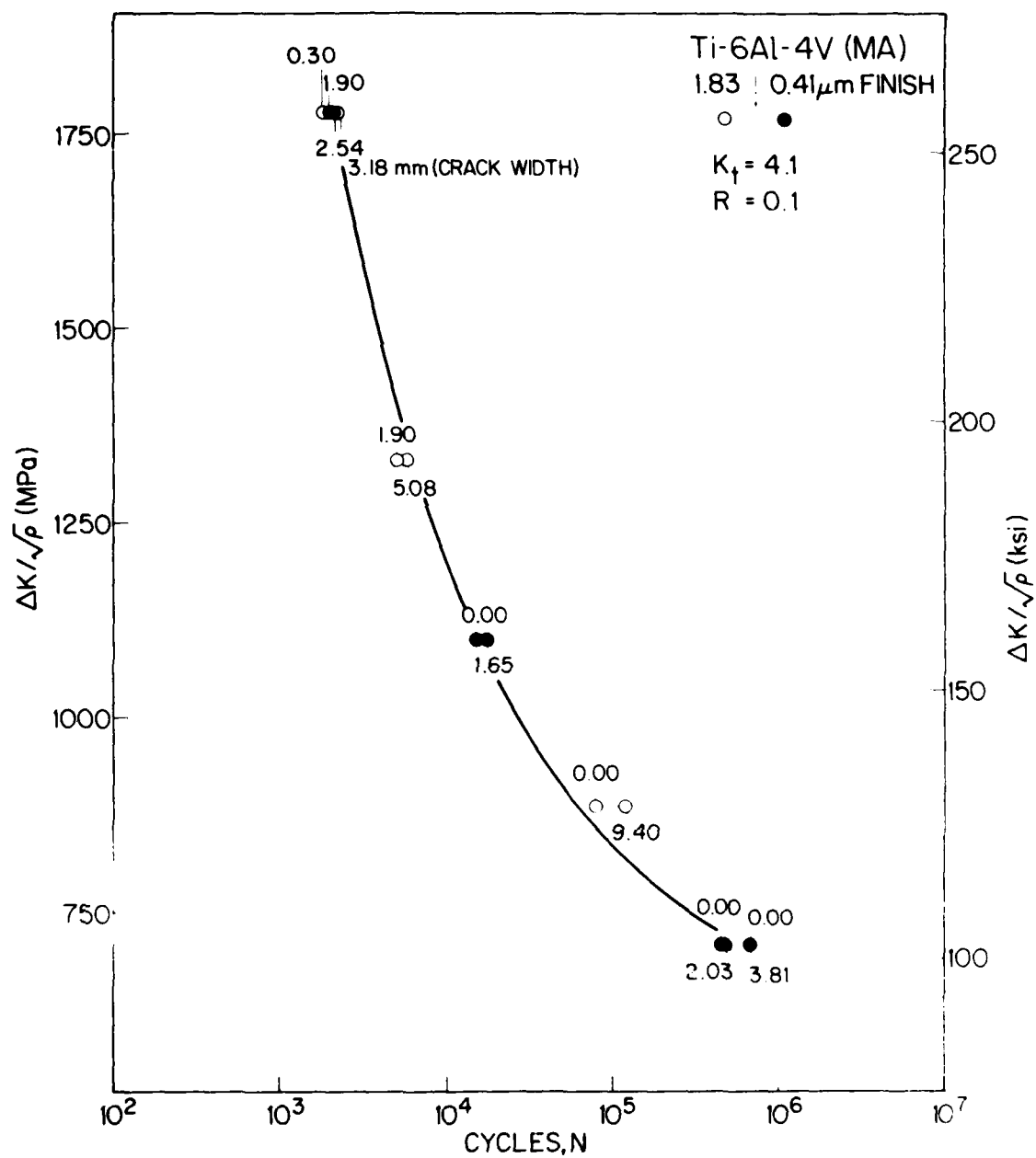
Fig. 3 - Fatigue-crack initiation data for the Ti-6Al-4V (MA) material. The two data points per specimen denote the smallest and largest crack sizes observed during testing.
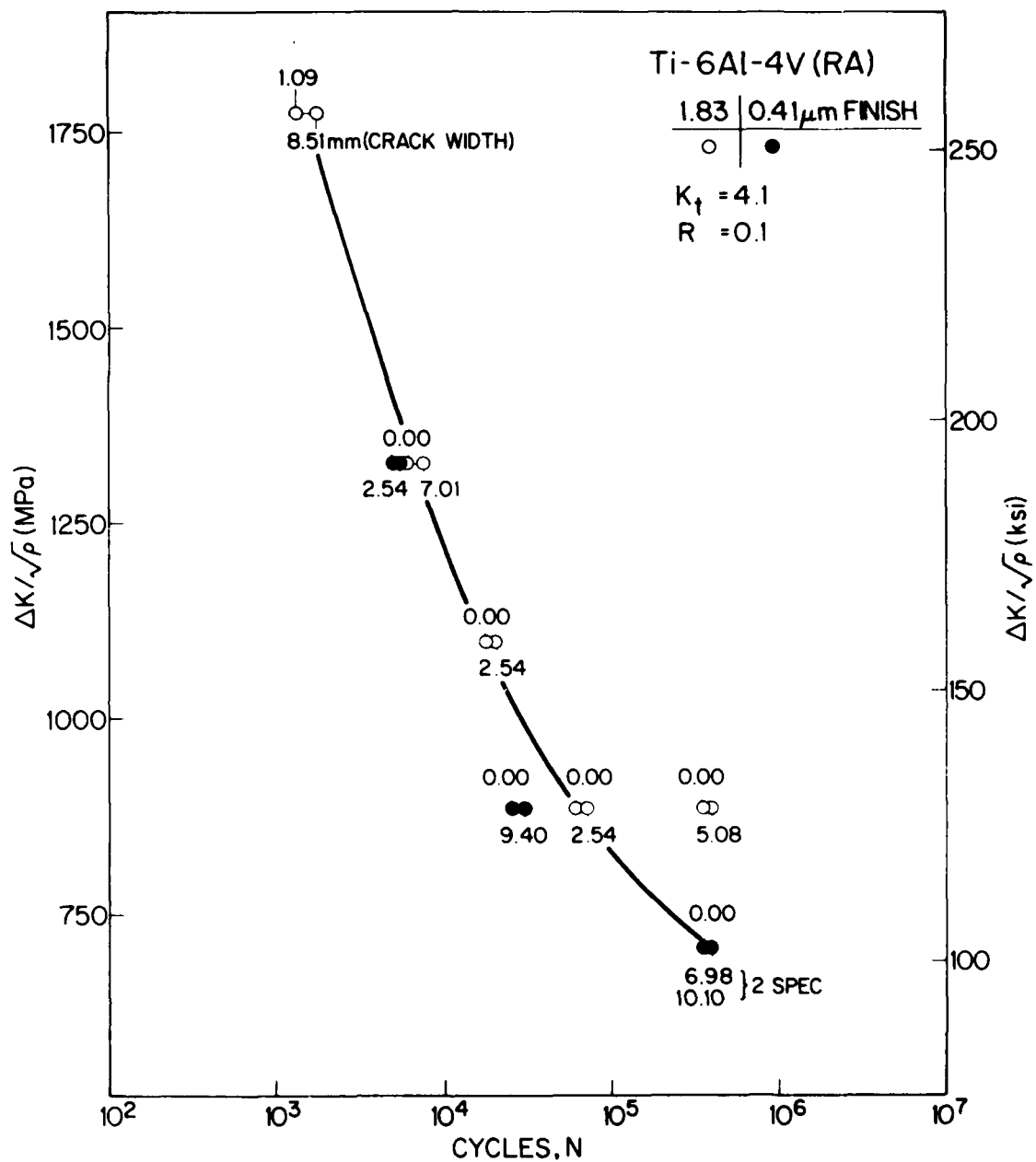
7

Fig. 4 - Fatigue-crack initiation data for the Ti-6Al-4V (RA) material.

Fig. 5 - Fatigue-crack initiation data for the Ti-6Al-4V (BA) material.

9

Two lots of crack initiation specimens were tested in the course of this investigation. In both lots, the notch root region was machined so as to produce tool marks oriented parallel to the principal tensile stress axis. The notch root surface of the first lot was machined to a 1.8 μm (72 μ-in.) finish. The notch roots of the second lot were honed to a noticeably smoother 0.4 μm (16 μ-in.) finish.

All fatigue tests, both crack initiation and crack propagation, were conducted in ambient room air. A sinusoidal waveform and a load ratio ($R = P_{min}/P_{max}$) of 0.1 was used throughout. Crack initiation tests were run at a cyclic frequency of 1 Hz. Crack propagation tests were run at 5 Hz.

RESULTS AND DISCUSSION

Results of the crack propagation tests are shown in Fig. 1, which contains a logarithmic plot of fatigue crack growth rate (da/dN) versus stress-intensity range (ΔK) for each of the three microstructures studied. The da/dN-versus-ΔK results show a distinct ordering on the basis of microstructure. The microstructural dependence of fatigue crack propagation in $\alpha + \beta$ titanium alloys has been the subject of considerable investigation by the authors in recent years as previously discussed in the Background section of this paper. The data shown in Fig. 1 are a typical example of the manner in which mean effective grain size ($\overline{\ell}$) controls da/dN-versus-ΔK relationships in this class of titanium alloys. Obviously grain size enlargement is very beneficial to crack propagation resistance; the focal point of this paper is to study what degree crack initiation resistance may be affected by increases in $\overline{\ell}$.

Results of the crack initiation tests are shown in Figs. 3-5. These are semilogarithmic plots of $\Delta K/\sqrt{\rho}$ versus cycles (N). A composite trend line summary of the data from Figs. 3-5 is given in Fig. 6. Each data point in Figs. 3-5 is denoted with a number indicating the observed crack length measured across the face of the notch root surface corresponding to the cycle count (N).

An examination of the $\Delta K/\sqrt{\rho}$-versus-N data shown in Figs. 3-5 reveals two salient points. First, in most instances, the number of elapsed cycles between no observable crack or a very small crack (~1 mm) and a crack which extends across a significant portion of the notch root face is relatively brief. Second, no difference could be seen in fatigue crack initiation behavior as a function of surface finish. Both of these observations are in good agreement with the experience of May et al. [18], who conducted a similar study of fatigue crack initiation in steels using blunt-notch fracture mechanics specimens.

10

Perhaps the most significant result of this investigation can be seen in the comparison of fatigue-crack initiation curves in Fig. 6. Here, the crack initiation resistance of the MA and RA materials appear indistinguishable. In the region $10^3 < N < 10^5$, the BA material's crack initiation resistance is somewhat inferior to the MA and RA materials. Beyond $N = 10^5$, all materials appear to be quite similar in their respective fatigue-crack propagation resistance, on the basis of the criteria employed in this investigation.

One final word as regards the influence of texture: From the modulus (E) data in Table 3, it is clear that materials associated with the MA and RA conditions exhibit a transverse texture, i.e., a preferential alignment of basal planes (of the α-phase) normal to the T direction. Thus - in view of the evidence in Ref. 10 - if the MA and RA conditions were tested in the orthogonal orientation, LT, one would expect poorer resistance in the high-cycle region than shown in Fig. 6 for the TL orientation, yet better resistance in the low-cycle region. On the other hand, the curve shown in Fig. 6 for the BA would not be expected to shift significantly for the orthogonal orientation, LT - inasmuch as similar moduli for the L and T directions reflect an equilibration of basal pole densities in the respective directions.

CONCLUSIONS

This investigation has examined the effects of microstructural modification on a broad range of strength, fatigue and crack-tolerance properties in a commercial purity Ti-6Al-4V alloy. The following conclusions have been reached from this work:

1) The principal microstructural parameter which affects the fatigue properties of Ti-6Al-4V materials is the mean effective grain size ($\bar{\ell}$).

2) Compared with the as-received MA material, the RA heat treatment resulted in a modest enhancement in fatigue-crack propagation resistance and no apparent change in fatigue-crack initiation resistance.

3) Compared with the as-received MA material, the BA heat treatment significantly enhanced fatigue-crack propagation resistance; however, for fatigue lives involving less than 10^5 cycles, the fatigue-crack initiation resistance for the BA material was moderately inferior to that of the MA and RA materials.

4) Both yield strength and fracture toughness were also affected by microstructural modification. The maximum degree of change in these properties occurred in comparisons between the MA and BA materials; K_{Ic} values for the BA material were double those for the MA material, but the yield strength decreased by approximately 15 percent.
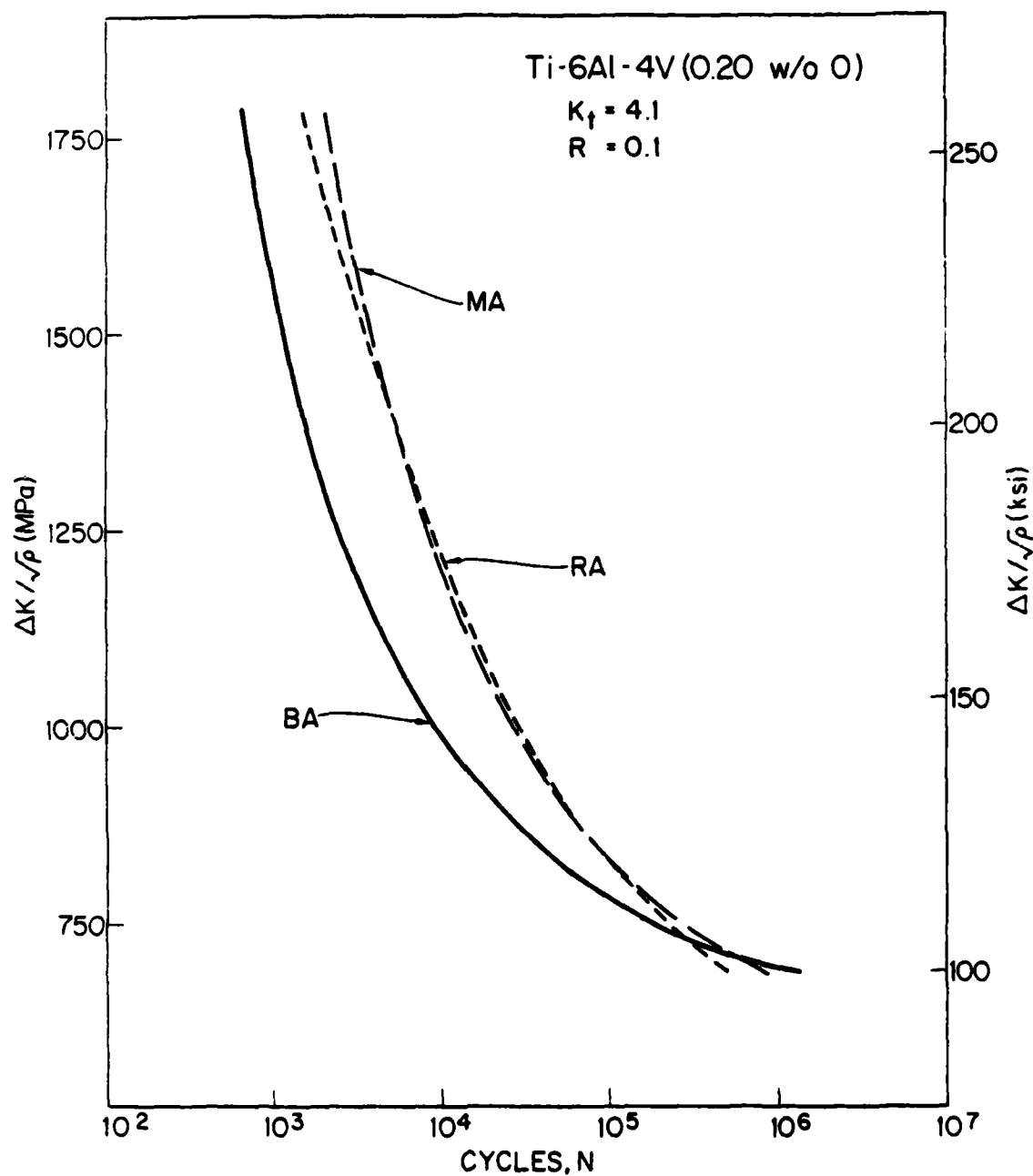
11

Fig. 6 - Summary of fatigue-crack initiation results for the three Ti-6Al-4V materials studied.

12

5) With the possible exception of low-cycle fatigue-crack initiation (i.e., less than 10^5 cycles), the BA material appears to offer the optimum combination of properties for critical applications involving fatigue and fracture considerations.

ACKNOWLEDGMENT

REFERENCES

1. G. R. Yoder, L. A. Cooley and T. W. Crooker, "Enhancement of Fatigue Crack Growth and Fracture Resistance in Ti-6Al-4V and Ti-6Al-6V-2Sn Through Microstructural Modification", Journal of Engineering Materials and Technology, Vol. 99, October 1977, pp. 313-318

2. M. A. Greenfield, C. M. Pierce and J. A. Hall, "The Effect of Microstructure on the Control of Mechanical Properties in Alpha-Beta Titanium Alloys", Titanium Science and Technology, Edited by R. I. Jaffee and H. M. Burte, Plenum Press, New York, 1973, Vol. 3, pp. 1731-1743

3. R. A. Sprague, D. L. Ruckle and M. P. Smith, "The Effect of Microstructure on the Low Cycle Fatigue Behavior of Ti-6Al-4V", ibid., pp. 2069-2079

4. J. J. Lucas, "Improvements in the Fatigue Strength of Ti-6Al-4V Forgings", ibid., pp. 2081-2095

5. A. W. Bowen and C. A. Stubbington, "The Effect of $\alpha + \beta$ Working on the Fatigue and Tensile Properties of Ti-6Al-4V Bars", ibid., pp. 2097-2108

6. C. A. Stubbington, "Metallurgical Aspects of Fatigue and Fracture in Titanium Alloys", Alloy Design for Fatigue and Fracture Resistance, AGARD Conference Proceedings No. 185, 1976, pp. 3-1 - 3-19

7. N. E. Paton, J. C. Williams, J. C. Chesnutt and A. W. Thompson, "The Effects of Microstructure on the Fatigue and Fracture of Commercial Titanium Alloys", ibid., pp. 4-1 - 4-14

8. M. Peters, A. Gysler and G. Lütjering, "Influence of Microstructure on the Fatigue Behavior of Ti-6Al-4V", Titanium '80, Edited by H. Kimura and O. Izumi, TMS-AIME, Warrendale, Pa., 1980, Vol. 3, pp. 1777-1786

9. G. R. Yoder, L. A. Cooley and T. W. Crooker, "Observations on the Generality of the Grain-Size Effect on Fatigue Crack Growth in $\alpha + \beta$ Titanium Alloys", ibid., pp. 1865-1873

10. F. Larson and A. Zarkades, "Properties of Textured Titanium Alloys", MCIC Report 74-20, Columbus, Ohio, June 1974

11. E 399-78a, "Standard Test Method for Plane-Strain Fracture Toughness of Metallic Materials", 1980 Annual Book of ASTM Standards, Part 10, American Society for Testing and Materials, 1980, pp. 580-601

12. E 647-78T, "Tentative Test Method for Constant-Load-Amplitude Fatigue Crack Growth Rates Above 10^{-8} m/Cycle", ibid., pp. 749-767

13. E 8-79a, "Standard Methods of Tension Testing of Metallic Materials", ibid., pp. 197-216

14. J. M. Barsom and R. C. McNicol, "Effect of Stress Concentration on Fatigue-Crack Initiation in HY-130 Steel", Fracture Toughness and Slow Stable Cracking, ASTM STP 559, American Society for Testing and Materials, 1974, pp. 183-204

15. W. G. Clark, Jr., "Evaluation of the Fatigue Crack Initiation Properties of Type 403 Stainless Steel in Air and Steam Environments", ibid., pp. 205-224

16. S. T. Rolfe and J. M. Barsom, Fracture and Fatigue Control in Structures, Prentice-Hall, Englewood Cliffs, N.J., 1977

17. N. E. Dowling, W. R. Brose and W. K. Wilson, "Notched Member Fatigue Life Predictions by the Local Strain Approach", Fatigue Under Complex Loading - Analysis and Experiments, Society of Automotive Engineers, Warrendale, Pa., 1977, pp. 55-84

18. R. A. May, A. Stuber and S. T. Rolfe, "Effective Utilization of High Yield Strength Steels in Fatigue", Welding Research Council Bulletin 243, New York, November 1978

19. V. J. Parks and R. J. Sanford, "Photoelastic and Holographic Analysis of a Turbine-Engine Component", Experimental Mechanics, Vol. 18, September 1978, pp. 328-334